Molecular Vision 2026; 32:34-47 <http://www.molvis.org/molvis/v32/34>
Received 2 June 2025 | Accepted 2 February 2026 | Published 4 February 2026

Molecular responses of human retinal pigment epithelial cells to ebolavirus VP24

Liam M. Ashander,[1] Yuefang Ma,[1] Genevieve F. Oliver,[1] Binoy Appukuttan,[1] Cameron D. Haydinger,[1] Steven Yeh,[2] Glenn A. Marsh,[3] Justine R. Smith[1]

(Last two authors contributed equally to this work and share last authorship.)

[1]Flinders Health and Medical Research Institute and College of Medicine and Public Health, Flinders University, Adelaide, Australia; [2]Truhlsen Eye Institute and Department of Ophthalmology, University of Nebraska Medical Center, Omaha, NE; [3]Australian Centre for Disease Preparedness, Health and Biosecurity, Commonwealth Scientific and Industrial Research Organisation, Geelong, Australia

Purpose: Uveitis (inflammation inside the eye) is a disabling manifestation of the post-Ebola syndrome that affects 10% to 35% of individuals who survive the infection. Post-Ebola uveitis presents with diverse clinical features but frequently involves the posterior segment of the eye, where the retinal pigment epithelium plays a key role in directing immune responses. Our previous work shows that this epithelium is relatively susceptible to infection with *Zaire ebolavirus* (EBOV), the strain responsible for most Ebola outbreaks. In addition to production roles, viral proteins may act to alter the molecular responses of host cells.

Methods: We investigated the activity of EBOV viral protein 24 (VP24) in human retinal pigment epithelial cells. An EBOV VP24 expression plasmid was constructed in-house. Multiple primary cell isolates were lipofectamine-transfected, first with VP24 or control expression plasmids and then with polyinosinic-polycytidylic acid (poly I:C) to simulate viral RNA. A type I interferon (IFN) response to transfection was confirmed by an IFN-β enzyme-linked immunosorbent assay. Cellular immune responses after 4- and 24-h exposures to poly I:C were characterized by reverse transcription-quantitative polymerase chain reaction.

Results: Multidimensional scaling, drawing on 19 immune response–related gene transcripts, covering antiviral, immunomodulatory, and proinflammatory molecules, demonstrated changes in gene expression profiles following transfection. Analysis of individual cell isolates showed a range of changes, including upregulation and downregulation of different gene transcripts across the two investigated time points.

Conclusions: Our findings suggest VP24 elicits variable immune responses from human retinal pigment epithelial cells, potentially contributing to the variation in clinical presentations of uveitis in Ebola survivors.

Since the first recognition of Ebola virus disease in 1976 in the Democratic Republic of the Congo, when *Zaire ebolavirus* (EBOV) infection resulted in 318 cases with an 88% fatality, there have been numerous outbreaks in African nations [1]. The largest of these was the 2014–2016 West African outbreak, based across Guinea, Liberia, and Sierra Leone: there were 28,610 reported cases of EBOV infection, and the case fatality rate was 39% [1]. This "West African Epidemic" has underpinned substantial new knowledge of the clinical course of the infectious disease, including recognition of a post-Ebola syndrome, associated with persistence of live virus in immune-privileged organs [2,3]. Epidemiological studies of Ebola survivors show that one of the most common and disabling post-Ebola conditions is uveitis (inflammation inside the immune-privileged eye), reported in up to approximately one-third of survivors [2-4]. This form of uveitis may be aggressive, illustrated by an early report of Ebola survivors in Liberia: 39% of affected eyes experienced blindness according to the World Health Organization classification [5].

The posterior segment of the eye is often involved clinically in Ebola-associated uveitis [6]. Different retinal and chorioretinal lesions have been reported, including some that appear common to intraocular infections by multiple pathogens and others that may be specific for ebolavirus infection [7,8]. Pathological changes in the outer retina have been demonstrated in these lesions by optical coherence tomography [9]. The retinal pigment epithelium abuts the outer retina, where it plays a key role in directing immune responses in the posterior eye [10], with a capacity to limit or promote inflammation in different infections [11–14]. Previously, we have shown that primary human retinal pigment epithelial cells are relatively susceptible to infection with EBOV [15].

The *Ebolavirus* genus belongs to the *Filoviridae* family of lipid-enveloped, negative-stranded RNA viruses [16].

Correspondence to: Justine R. Smith, Health and Medical Research Building, Flinders University, Flinders Drive, Bedford Park, SA 5042, Australia; email: justine.smith@flinders.edu.au

Ebola viruses replicate rapidly in permissive cells, primarily by limiting the type I interferon (IFN) response [17], a critical innate immune defense against viral infections [18]. Studies conducted in rhesus macaques suggest that IFN-β is largely responsible for the response to EBOV [19]. Several structural viral proteins act to block the host cell type I IFN response. In particular, viral protein 24 (VP24) binds importin proteins that are responsible for shuttling activated signal transducer and activator of transcription 1 (STAT1) to the nucleus, thereby inhibiting transcription of IFN-stimulated genes [20]. The ARPE-19 human retinal pigment epithelial cell line generates a strong type I IFN response following EBOV infection, suggesting this cell population has the capacity to control viral replication and potentially act as an intraocular viral reservoir [21]. However, the ARPE-19 cell line differs considerably phenotypically from primary human retinal pigment epithelial cells [22].

The VP24 protein sequence differs across the species of Ebolavirus species, with implications for the pathogenesis of the infectious disease [23]. In this work, we investigated the activity of EBOV VP24 in primary human retinal pigment epithelial cells. Cell isolates, prepared in-house, were transfected first with the VP24 expression plasmid and subsequently with polyinosinic-polycytidylic acid (poly I:C) to model infection with VP24-expressing RNA virus; antiviral, immunomodulatory, and proinflammatory cellular responses were studied by reverse transcription-quantitative polymerase chain reaction (RT-qPCR).

METHODS

Human retinal pigment epithelial cell isolation and culture: Retinal pigment epithelial cells were isolated from posterior eyecups of human cadaveric donors using a method we have published previously, which yields cells that express specific proteins, including cellular retinaldehyde-binding protein, cytokeratin 8, retinal pigment epithelium–specific 65 kDa protein, and zonula occludens 1, and do not express α–smooth muscle actin, a marker of mesenchymal differentiation (Figure 1A) [24]. Briefly, the retinal pigment epithelium was peeled from the posterior eyecups, enzymatically digested using 0.25 mg/ml collagenase IA/collagenase IV (Merck-Sigma Aldrich, St. Louis, MO) for 30 min at 37 °C and 5% CO_2 in air, and purified by sucrose density gradient centrifugation. Isolated cells were grown to confluence in 50% minimum essential medium (Eagle's modification), 25% Dulbecco's modified Eagle's medium, and 25% Ham's F-12 medium (F12) with 1× N1 Medium Supplement, 1× Non-Essential Amino Acids Solution, 1× GlutaMAX Supplement, 0.25 mg/ml taurine, 0.02 µg/ml hydrocortisone, 0.013 ng/ml 3,3′,5-triiodo-L-thyronine sodium, and 100 U/ml penicillin-streptomycin (all obtained from Merck-Sigma Aldrich or Thermo Fisher Scientific–GIBCO, Grand Island, NY), as well as 10% fetal bovine serum (Thermo Fisher Scientific–GIBCO), and frozen in liquid nitrogen ahead of use in the plasmid transfection experiments.

Construction and characterization of Zaire ebolavirus viral protein 24 expression plasmid: Zaire ebolavirus VP24 coding sequence was inserted into a FLAG-tagged mammalian expression plasmid for constitutive expression under the control of the chicken β-actin promoter and enhancer (pCAGGS-FLAG). The VP24 coding sequence was amplified using Q5 Hot Start High-Fidelity Polymerase (New England Biolabs, Ipswich, MA) with flanking primers containing restriction enzyme sites for NotI and NheI (F: 5′-TTT CGA GCG CGG CCG CAA TGG CTA AAG CTA GGG GAC G-3′, R: 5′-AAA GAT CTG CTA GCG TTA GAT AGC AAG AGA GCT A-3′). Amplified sequence and pCAGGS-FLAG were double-digested with NotI and NheI restriction enzymes (New England Biolabs), purified, and ligated in-frame downstream of the FLAG sequence using T5 DNA Ligase (New England Biolabs). The pCAGGS-FLAG-VP24 plasmid was purified using the Genelute HP Endotoxin-Free Plasmid Maxi-Prep Kit (Merck–Sigma Aldrich), and the VP24 coding sequence was confirmed by Sanger sequencing and alignment to the EBOV isolate Ebola virus/*Homo sapiens*-tc/COD/1976/Yambuku-Mayinga (GenBank: MK114118.1). Western blot of protein extract from ARPE-19 cells (American Type Culture Collection, Manassas, VA) that were lipofectamine-transfected with pCAGGS-FLAG-VP24 was performed to confirm VP24 expression. Protein extract was run on a 12% polyacrylamide gel and probed with anti–EBOV VP24 (Sino Biological, Beijing, China; catalog number: 40454-T4) at a 1:3,000 dilution.

Plasmid and polyinosinic-polycytidylic acid transfection of retinal pigment epithelial cells: Retinal pigment epithelial cells (passage 2) were grown to confluence in 24-well plates (growth area 1.9 cm^2) and maintained for approximately 2 weeks at 37 °C and 5% CO_2 in air, in the standard culture medium. Immediately before cell transfection, the medium was refreshed with 500 µl per well. Individual wells of cells were transfected with 0.8 µg VP24 expression plasmid or negative control plasmid with no insert, complexed with 2 µl Lipofectamine 2000 (Thermo Fisher Scientific–Life Technologies, Vilnius, Lithuania) in 100 µl Opti-MEM I Reduced Serum Medium (Thermo Fisher Scientific–GIBCO). A pMAX-GFP expression plasmid (Lonza, Walkersville, MD) was similarly delivered to additional wells to confirm cell transfection. After a 48-h incubation at 37 °C and 5% CO_2 in

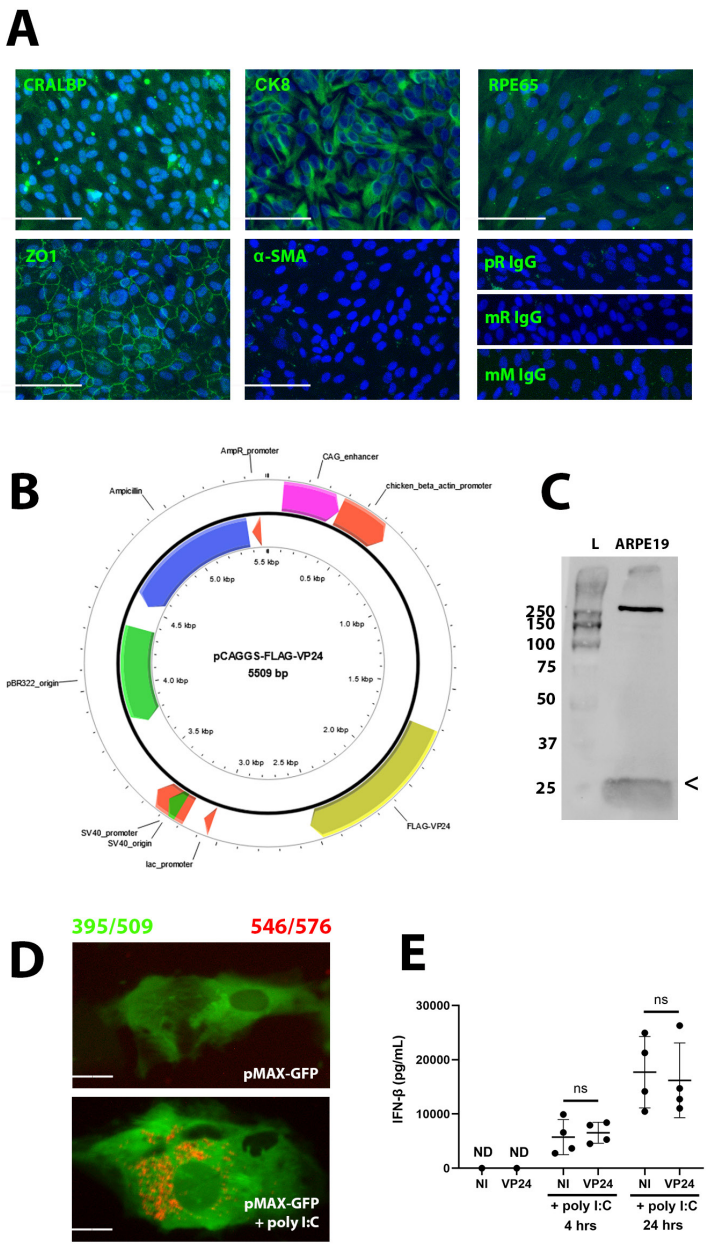

Figure 1. Characterization of human retinal pigment epithelial cells, pCAGGS-FLAG-VP24 expression plasmid, and transfection procedures. **A**: Fluorescent photomicrographs of retinal pigment epithelial cells (isolate 4) immunophenotyped for five markers (cellular retinaldehyde-binding protein [CRALBP], cytokeratin 8 [CK8], retinal pigment epithelium–specific 65 kDa protein [RPE65], zonula occludens 1 [ZO], α–smooth muscle actin [α-SMA]) or species- and isotype-matched control antibodies (polyclonal rabbit IgG [pR IgG], monoclonal rabbit IgG [mR IgG], monoclonal mouse IgG1k [mM IgG]), with 4′,6-diamidino-2-phenylindole (DAPI) nuclear counterstain. Original magnification = 200×; scale bar = 100 µm. **B**: Schematic representation of the pCAGGS-FLAG-VP24 expression plasmid generated using PlasMapper version 3.0. **C**: Western blot of *Zaire ebolavirus* viral protein 24 (VP24) in protein extracted from ARPE-19 cells transfected with pCAGGS-FLAG-VP24 (arrowhead = expected molecular weight, 29 kDa). Ladder (L) molecular weight standards are in kDa. **D**: Fluorescent photomicrograph showing a retinal pigment epithelial cell transfected with green fluorescent protein (GFP) expression vector plus or minus rhodamine-labeled (Rho) polyinosinic-polycytidylic acid (poly I:C). Original magnification = 400×; scale bar = 50 µm. **E**: Interferon-β (IFN-β) concentration measured in culture supernatant after cellular transfection with VP24 or no-insert control (NI) expression plasmid for 48 h, followed by poly I:C for an additional 4 or 24 h (hours) by enzyme-linked immunosorbent assay. An additional control replacing poly I:C with water was included for the 4-h condition. Circles represent mean protein concentration for individual cell isolates, crossbars indicate mean, and error bars indicate standard deviation (n = 4 isolates/condition). ND, 2 of 4 isolates below detection limit (7.8 pg/ml); ns, not significant.

air, each well of cells was transfected again, now with 0.5 µg each of high and low molecular weight poly I:C (Invivogen, San Diego, CA), complexed with 2 µl Lipofectamine 2000 in 100 µl Opti-MEM I Reduced Serum Medium. After a further 4 or 24 h of incubation at 37 °C and 5% CO_2 in air, the cell culture supernatant was collected from the wells and stored at −80 °C for use in an enzyme-linked immunosorbent assay (ELISA). The cells were then covered with RLT lysis buffer (Qiagen, Hilden, Germany), and the plates were placed at −80 °C for later extraction of RNA.

Interferon-β ELISA: Cell culture supernatants were thawed on ice and assayed in duplicate for IFN-β using the quantitative sandwich ELISA (CUSABIO, Wuhan, China; catalog number: CSB-E09889h) according to the manufacturer's instructions. Absorbance was read on the Victor X3 multilabel plate reader (PerkinElmer, Waltham, MA), and IFN-β concentration was interpolated by four-parameter logarithm standard curve fitting, using WorkOut software version 2.5 (PerkinElmer). The absolute limit of detection for the ELISA was 7.8 pg/ml.

RNA extraction and reverse transcription: RNA was extracted from transfected retinal pigment epithelial cells using the RNeasy Mini Kit with optional on-column DNase I digest (Qiagen) according to the manufacturer's instructions. RNA concentration was measured by spectrophotometry using the Nanodrop 2000 (Thermo Fisher Scientific, Wilmington, DE). Synthesis of cDNA was performed using iScript Reverse Transcription Supermix for RT-qPCR (Bio-Rad, Hercules, CA), with 100 to 250 ng RNA input resulting in 20 µl cDNA. Duplicate synthesis reactions were prepared for each sample, pooled, and diluted 10-fold for use in the qPCR.

Quantitative polymerase chain reaction: The qPCR was performed on the CFX Connect Real-Time PCR Detection System (Bio-Rad) using 2 µl diluted cDNA, 10 µl SsoAdvanced SYBR Green Supermix (Bio-Rad), 0.75 µl each of 10 µM forward and reverse primers (Merck–Sigma Aldrich–Genosys, The Woodlands, TX), and nuclease-free water for each reaction. Primer sequences and expected product sizes are presented in Table 1 and Appendix 1. The amplification consisted of a precycling hold at 95 °C for 30 s, 40 cycles of denaturation at 95 °C for 30 s, annealing at 60–62 °C for 30 s, and extension at 72 °C for 30 s. A melting curve, representing a 1-s hold at every 0.5 °C between 70 °C and 95 °C, was generated to confirm that each primer set produced a single peak. Primer efficiency for all primer sets was 80% or greater. The amplicon size of each qPCR product was confirmed by electrophoresis on 2% agarose gel. The cycle threshold was measured with Cq determination mode set to regression (CFX Manager version 3.1; Bio-Rad). Relative expression, normalized to the geometric mean of two stable reference genes, peptidylprolyl isomerase A and glyceraldehyde-3-phosphate dehydrogenase, was determined using the method described by Pfaffl [25]. Immune response–related gene transcripts were selected for measurement primarily on the basis of previous work describing human retinal pigment epithelial cell responses to infection with EBOV [21] and other microbial pathogens [26–28].

Statistical analyses: Data were analyzed using GraphPad Prism (version 9.0.0; GraphPad Software, La Jolla, CA). Comparisons between two conditions for individual isolates were made using the unpaired two-tailed Student *t* test. Welch's correction was applied to comparisons where the *F* test indicated variances were unequal. Comparisons between two conditions using means of all isolates were made by a paired two-tailed Student *t* test. A statistically significant difference was defined by a *p* value of less than 0.05 for all comparisons. Multidimensional scaling was performed in R version 4.4.1 using the plotMDS function of R package limma version 3.60.4.

Research compliance: Posterior eyecups of human cadaveric donors were provided by the Eye Bank of South Australia (Adelaide, Australia). Use of the eye tissue for this research was approved by the Southern Adelaide Clinical Human Research Ethics Committee (Protocol number: 175.13). Informed consent for participation did not apply because the participants were deceased. Next of kin gave consent for the research use of eye tissue that otherwise would have been discarded after utilization of the donor eyes in the corneal transplantation program. Cloning and use of EBOV VP24 plasmid for the work was approved by the Flinders University Institutional Biosafety Committee (Dealing 2023–12). All experiments were performed in accordance with relevant local guidelines and regulations.

RESULTS

The primary human retinal pigment epithelial cell isolates used in this work were prepared from posterior eyecups of five male and five female cadaveric donors. Age at death ranged from 41 to 80 years (median = 62 years). Death-to-processing time ranged from 18.5 to 46.5 h (median = 26.5 h).

Sequencing confirmed insertion of VP24 in-frame with FLAG in pCAGGS-FLAG-VP24 (Figure 1B), and a western blot for VP24 in plasmid-transfected ARPE-19 cells indicated expression (Figure 1C). For transfection experiments using primary human retinal pigment epithelial cell isolates, transfection efficiency was 50% or greater, estimated on the percentage of cells expressing green fluorescent protein in wells transfected with pMAX-GFP (Figure

Table 1. Sequences and amplicon sizes of primer pairs used in quantitative polymerase chain reactions.

Gene transcript [Reference]	Primer sequences (5'-3')	Size (bp)	NCBI accession number
Immune Response			
CCL2	F: GCATGAAAGTCTCTGCCGC R: GGACACTTGCTGCTGGTGATT	181	NM_002982.4
CD274 [49]	F: ACGCATTTACTGTCACGGTTCC R: GACTTCGGCCTTGGGGTAGC	446	NM_014143.4
EIF2AK2 [50]	F: GGAAAGCGAACAAGGAGTAAGG R: CCAAAGCGTAGAGGTCCACT	97	NM_002759.4
ICAM1 [51]	F: TAAGCCAAGAGGAAGGAGCA R: CATATCATCAAGGGTTGGGG	289	NM_000201.3
IFIT1 [52]	F: AGAAGCAGGCAATCACAGAAAA R: CTGAAACCGACCATAGTGGAAAT	112	NM_001548.5
IFITM1 [53]	F: ACTCCGTGAAGTCTAGGGACA R: TGTCACAGAGCCGAATACCAG	155	NM_003641.5
IL1B [49]	F: TGACCTGAGCACCTTCTTTC R: CAGCTGTAGAGTGGGCTTATC	331	NM_000576.3
IL1RN [54]	F: TCATGCTCTGTTCTTGGGAAT R: GCTTGTCCTGCTTTCTGTTC	131	NM_173842.3
IL6 [55]	F: ATGCAATAACCACCCCTGACC R: CCATGCTACATTTGCCGAAGAG	160	NM_00600.5
ISG15 [56]	F: GAGAGGCAGCGAACTCATCT R: AGCATCTTCACCGTCAGGTC	99	NM_005101.4
MX1 [57]	F: ACAATCAGCCTGGTGGTGGTC R: CCTCCCCTACAGTTTCCTCTCC	565	NM_001144925.2
OAS1 [57]	F: AGGTGGTAAAGGGTGGCT R: TGCTTGACTAGGCGGATG	472	NM_016816.4
PDCD1LG2 [58]	F: CAACTTGGCTGCTTCACATTTT R: TGTGGTGACAGGTCTTTTTGTTGT	137	NM_025239.4
RIGI [59]	F: GACTGGACGTGGCAAAACAA R: TTGAATGCATCCAATATACACTTCTG	75	NM_014314.4
RSAD2 [60]	F: TGACGGAACAGATCAAAGCA R: GCACCAAGCAGGACACTTCT	174	NM_080657.5
TGFB1	F: CGTGGAGCTGTACCAGAAATAC R: CGTGGAGCTGAAGCAATAGT	367	NM_000660.7
TGFB2	F: GTACTACGCCAAGGAGGTTTAC R: TGTGGAGGTGCCATCAATAC	568	NM_001135599.2
TNF [61]	F: TCTCGAACCCCGAGTGACAA R: TGAAGAGGACCTGGGAGTAG	181	NM_000594.4
VCAM1	F: GGATGCAGACAGGAAGTCCC R: GCTGGAACAGGTCATGGTCA	247	NM_001078.4
Reference			
GAPDH [62]	F: AGCTGAACGGGAAGCTCACTGG R: GGAGTGGGTGTCGCTGTTGAAGTC	209	NM_002046.7
PPIA [28]	F: GAGCACTGGAGAGAAAGGATTT R: GGTGATCTTCTTGCTGGTCTT	355	NM_021130.5

EIF2AK2=eukaryotic translation initiation factor 2 alpha kinase 2, GAPDH=glyceraldehyde-3-phosphate dehydrogenase, ICAM1=intercellular adhesion molecule 1, IFIT1=interferon induced protein with tetratricopeptide repeats 1, IFITM=interferon induced transmembrane protein 1, IL1B=interleukin 1 beta, IL1RN=interleukin 1 receptor antagonist, IL6=interleukin 6, ISG15=ISG15 ubiquitin like modifier, MX1=MX dynamin like GTPase 1, OAS1=2'-5'-oligoadenylate synthetase 1, CD274=CD274 molecule (programmed death-ligand 1), PDCD1LG2=programmed cell death 1 ligand 2, PPIA=peptidylprolyl isomerase A, RIGI=RNA sensor RIG-I, RSAD2=radical S-adenosyl methionine domain containing 2, TGFB1=transforming growth factor beta 1, TGFB2=transforming growth factor beta 2, TNF=tumor necrosis factor, VCAM1=vascular cell adhesion molecule 1. Primers designed in-house and amplicons confirmed by sequencing.

1D). An ELISA confirmed induction of IFN-β in cell isolates transfected with pCAGGS-FLAG-VP24 or pCAGGS-FLAG following a second transfection with poly I:C. As expected, given VP24 acts downstream of IFN-β, there was no significant difference in the level of IFN-β protein induced in VP24 versus no expression conditions, 4 or 24 h after the poly I:C transfection (Figure 1E).

The response of poly I:C-stimulated human retinal pigment epithelial cells to VP24 was examined by measuring expression of 19 immune-related gene transcripts, including eight antiviral (i.e., EIF2AK2, IFIT1, IFITM, ISG15, MX1, OAS1, RIGI, RSAD2), five immunomodulatory (i.e., CD274, IL1RN, PDCD1LG2, TGFB1, TGFB2), and six proinflammatory (i.e., CCL2, ICAM1, IL1B, IL6, TNF, VCAM1), by RT-qPCR. Multidimensional scaling was performed to assess the influence of VP24 on overall gene expression by individual retinal pigment epithelial cell isolates (Figure 2). At both 4 and 24 h, VP24 led to a change in gene expression in comparison to the no viral protein control condition, for each of the individual isolates (eight and six donors, respectively), and this effect was more obvious at 24 h. However, the effect was donor-dependent, and there was an obvious, strong influence of donor on overall gene expression that did not appear to be associated with either sex or age at death. These results imply VP24 alters the expression of immune-related gene transcripts in human retinal pigment epithelial cells, and the effect is highly donor-dependent.

The effect of VP24 on each of the immune-related gene transcripts was examined in the four retinal pigment epithelial cell isolates studied at 4 and 24 h after stimulation with poly I:C. Mean expression of eight antiviral transcripts did not differ significantly between the VP24 and no viral protein control conditions at either time point (Figure 3). However, there were significant changes in expression levels of six of the eight gene transcripts, including both induction and reduction, at one or other time point for individual cell isolates: EIF2AK2 (one donor, one time point), IFIT1 (one donor, two time points), ISG15 (three donors, one or two time points), OAS1 (one donor, one time point), RIGI (one donor, two time points), and RSAD2 (two donors, one time point). For one isolate, there was no change in expression of any antiviral transcripts; expression of one transcript changed in another isolate; and expression of four transcripts changed in the other two isolates.

Similar results were observed for the groups of immunomodulatory and proinflammatory gene transcripts. With one exception (IL1B), mean expression of five immunomodulatory and six pro-inflammatory transcripts did not differ significantly between the VP24 and no viral protein control conditions at 4 or 24 h (Figure 4 and Figure 5, respectively). Yet, when isolates were considered individually, there was a significant induction or reduction at one or other time point in four of five immunomodulatory transcripts (Figure 4): CD274 (one donor, one time point), PDCD1LG2 (three donors, one or two time points), TGFB1 (one donor, one time point), and TGFB2 (two donors, one time point), as well as five of six proinflammatory transcripts (Figure 5): CCL2 (three donors, one time point), ICAM1 (two donors, one or two time points), IL1B (one donor, one time point), IL6 (two donors, one or two time points), and VCAM1 (one donor, one time point). Expression of one transcript changed in one isolate, expression of five transcripts changed in another two isolates, and expression of six transcripts changed in the final isolate. Interestingly, the isolate that showed changes in six immunomodulatory or proinflammatory transcripts had no changes in antiviral transcripts.

The impact of VP24 on expression of transcripts encoding nuclear importers of STAT1 (i.e., KPNA1, KPNA5, and KPNA6 [29]), which are targets of VP24, was also examined in poly I:C–stimulated human retinal pigment epithelial cells. There were no significant expression differences at 4 h, but at 24 h, KPNA1 transcript increased in one isolate, and KPNA6 transcript increased in two isolates in the presence of VP24 (Appendix 2), suggesting the possibility of a feedback effect.

DISCUSSION

Apart from its role as a structural protein, EBOV VP24 has the potential to strongly block the type I IFN response in susceptible host cells. To evaluate its effect in the retinal pigment epithelium, a potential intraocular reservoir for EBOV, we constructed VP24 and control expression plasmids and used these to transfect primary human cell isolates. Cell transfection was repeated with poly I:C to simulate viral RNA, verified by secretion of IFN-β. Multidimensional

Abbreviations: CCL2=C-C motif chemokine ligand 2, EIF2AK2=eukaryotic translation initiation factor 2 alpha kinase 2, GAPDH=glyceraldehyde-3-phosphate dehydrogenase, ICAM1=intercellular adhesion molecule 1, IFIT1=interferon induced protein with tetratricopeptide repeats 1, IFITM=interferon induced transmembrane protein 1, IL1B=interleukin 1 beta, IL1RN=interleukin 1 receptor antagonist, IL6=interleukin 6, ISG15=ISG15 ubiquitin like modifier, MX1=MX dynamin like GTPase 1, OAS1=2'-5′-oligoadenylate synthetase 1, CD274=CD274 molecule (programmed death-ligand 1), PDCD1LG2=programmed cell death 1 ligand 2, PPIA=peptidylprolyl isomerase A, RIGI=RNA sensor RIG-I, RSAD2=radical S-adenosyl methionine domain containing 2, TGFB1=transforming growth factor beta 1, TGFB2=transforming growth factor beta 2, TNF=tumor necrosis factor, VCAM1=vascular cell adhesion molecule 1. □Primers designed in-house and amplicons confirmed by sequencing.

scaling, drawing on 19 immune response–related gene transcripts, covering antiviral, immunomodulatory, and proinflammatory molecules, showed a change in gene expression profile with transfection. Analysis of the data by individual cell isolates from four donors showed a range of significant changes between VP24 transfection and control conditions, including upregulation and downregulation of most gene transcripts across two investigated time points.

Viral protein 24 acts on type I IFN responses downstream of IFN production, and thus, as expected, it did not impact production of IFN-β by the expression plasmid-transfected retinal pigment epithelial cells. However, effects on

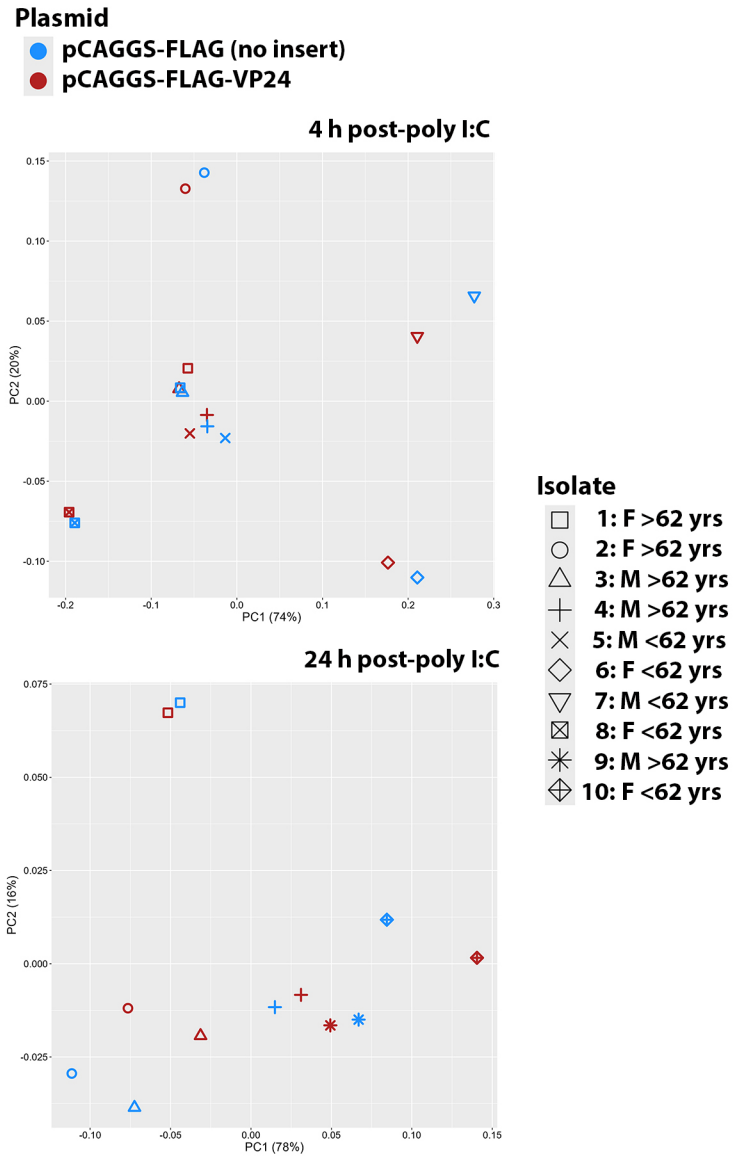

Figure 2. Multidimensional scaling of gene transcription in human retinal pigment epithelial cells. Plots show $\log_2$ fold differences for 19 immune response–related (antiviral, immunomodulatory, and proinflammatory) gene transcripts measured by quantitative polymerase chain reaction after transfection with *Zaire ebolavirus* viral protein 24 (VP24, red) or no-insert control (blue) expression plasmid for 48 h, followed by polyinosinic-polycytidylic acid (poly I:C) for an additional 4 or 24 h (hours). Symbols represent individual isolates, indicating gender and age at death dichotomized around the median of 62 years (yrs). M, male; F, female; PC (%), principal component (% variation).

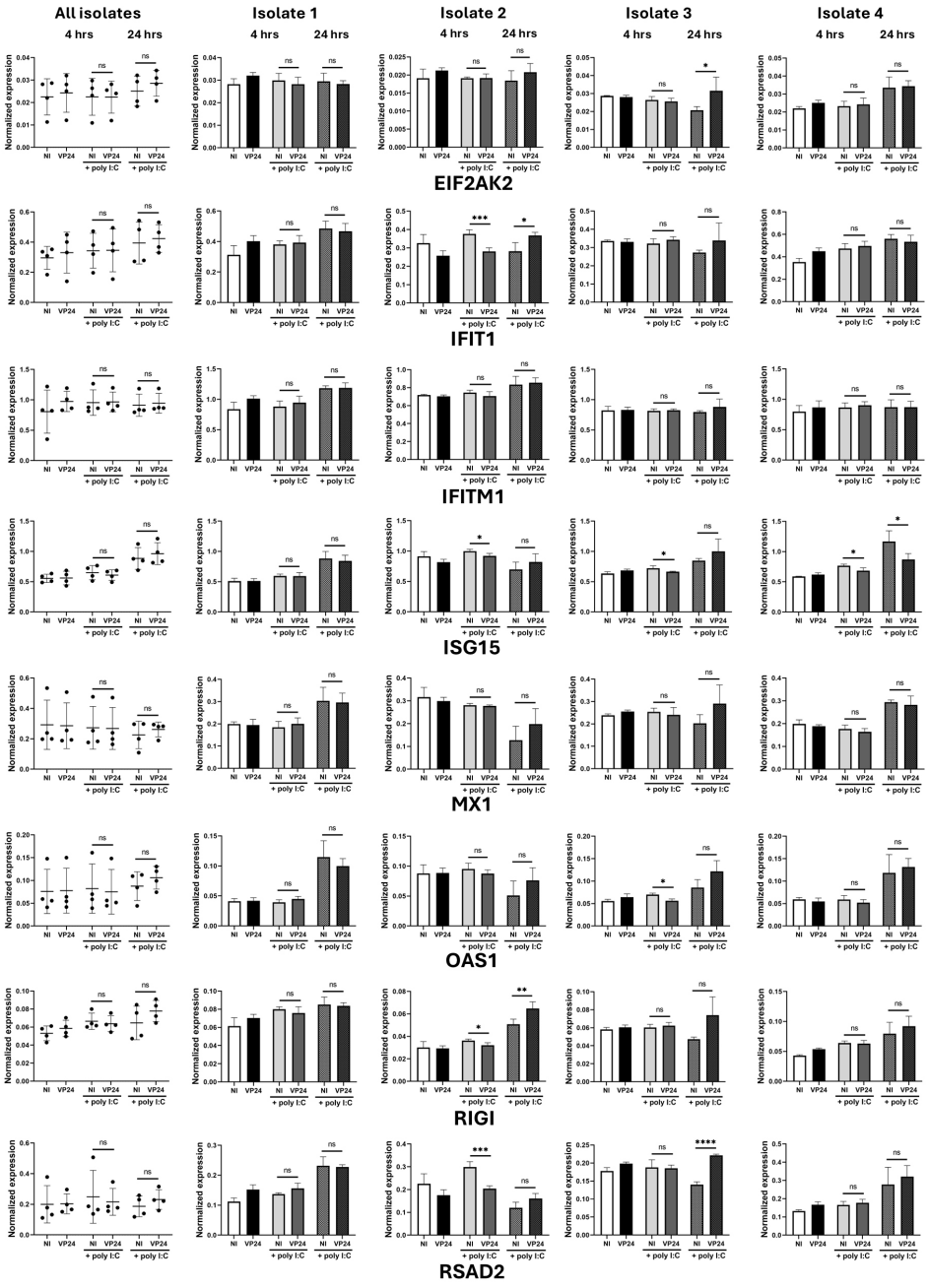

Figure 3. Expression of antiviral gene transcripts in human retinal pigment epithelial cells. After transfection with *Zaire ebolavirus* viral protein 24 (VP24) or no-insert control (NI) expression plasmid for 48 h, followed by polyinosinic-polycytidylic acid (poly I:C) for an additional 4 or 24 h (hours), cellular levels of eight antiviral transcripts were measured by quantitative polymerase chain reaction and normalized to two stable reference genes (glyceraldehyde 3-phosphate dehydrogenase [GAPDH] and peptidylprolyl isomerase A [PPIA]). An additional control replacing poly I:C with water was included for the 4-h condition. In *All Isolate* graphs, circles represent mean expression in individual isolates, crossbars indicate mean, and error bars indicate standard deviation (n = 4 isolates/condition). In *Isolate 1–4* graphs, bars indicate mean normalized expression, and error bars indicate standard deviation (n = 4 replicates/condition). EIF2AK2, eukaryotic translation initiation factor 2 alpha kinase 2; IFIT1, interferon-induced protein with tetratricopeptide repeats 1; IFITM1, interferon-induced transmembrane protein 1; ISG15, ISG15 ubiquitin-like modifier; MX1, MX dynamin-like GTPase 1; ns, not significant; OAS1, 2′-5′-oligoadenylate synthetase 1; RIGI, RNA sensor RIG-I; RSAD2, radical S-adenosyl methionine domain containing 2. *$p < 0.05$, **$p < 0.01$, ***$p < 0.001$, ****$p < 0.0001$.

expression of antiviral transcripts were also relatively limited, with changes in six of eight different molecules studied—EIF2AK2, IFIT1, ISG15, OAS1, RIGI, and RSAD2—but four in one isolate only and one isolate showing no change in any. These molecules have different functions in the type I IFN response: RIGI is a sensor for non-self, viral RNA motifs [30]; OAS1 and RSAD2 target viral RNA replication [31,32]; EIF2AK2 and IFIT1 inhibit viral RNA translation [33,34]; and ISG15 conjugates viral and host proteins to stall virus production [35]. These findings suggest VP24 has a modest blockade effect on the constitutive or induced expression of antiviral transcripts in human retinal pigment epithelial cells, which, by extrapolation, may moderately affect EBOV replication.

Transfection with VP24 also had an effect on the host cell inflammatory response, including some immunomodulatory and proinflammatory transcripts. Nine of 11 inflammatory

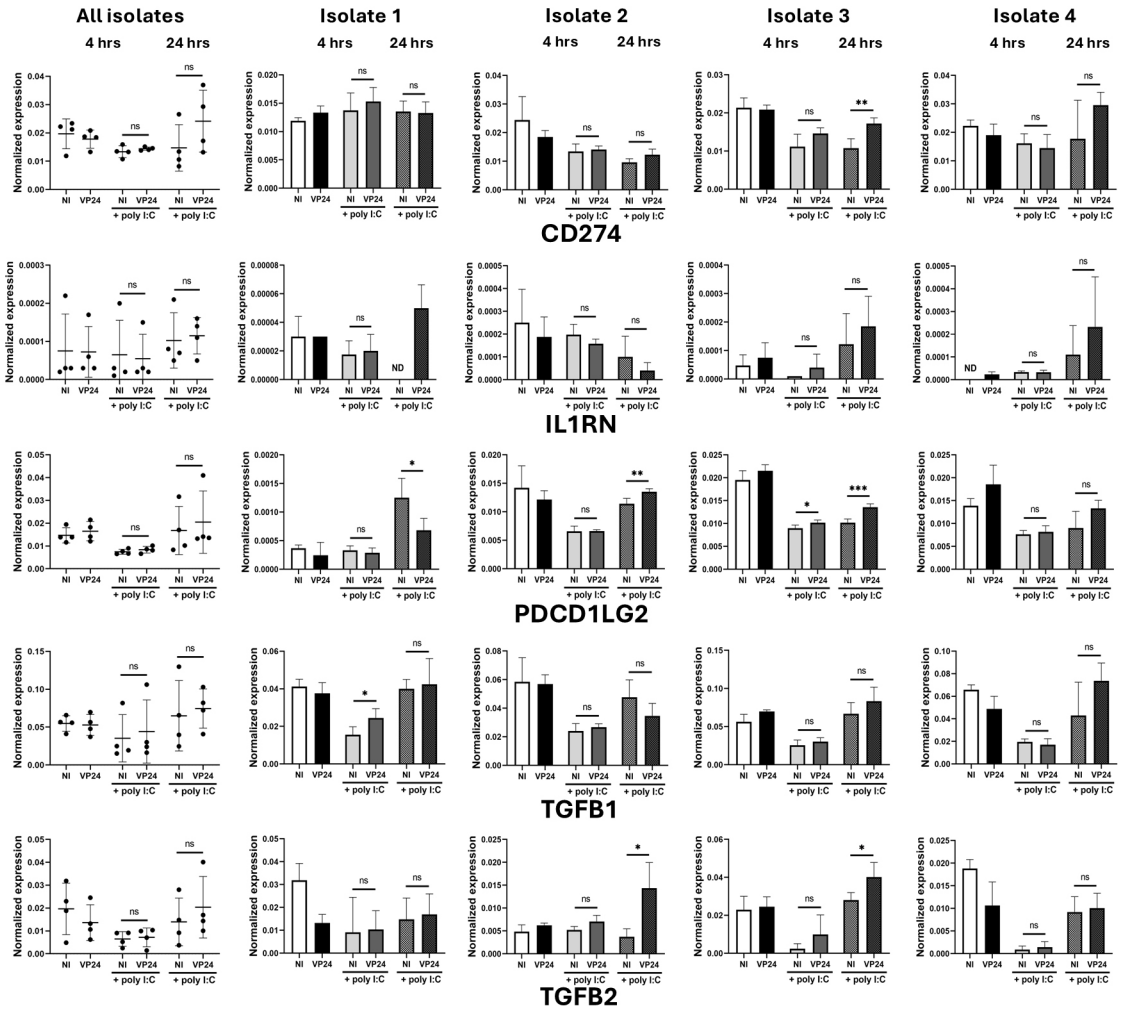

Figure 4. Expression of immunomodulatory gene transcripts in human retinal pigment epithelial cells. After transfection with *Zaire ebolavirus* viral protein 24 (VP24) or no-insert control (NI) expression plasmid for 48 h, followed by polyinosinic-polycytidylic acid (poly I:C) for an additional 4 or 24 h (hours), cellular levels of five immunomodulatory gene transcripts were measured by quantitative polymerase chain reaction and normalized to two stable reference genes (glyceraldehyde 3-phosphate dehydrogenase [GAPDH] and peptidylprolyl isomerase A [PPIA]). An additional control replacing poly I:C with water was included for the 4-h condition. In *All Isolate* graphs, circles represent mean expression in individual isolates, crossbars indicate mean, and error bars indicate standard deviation (n = 4 isolates/condition). In *Isolate 1–4* graphs, bars indicate mean normalized expression, and error bars indicate standard deviation (n = 4 replicates/condition). CD274, CD274 molecule (programmed death-ligand 1); IL1RN, interleukin 1 receptor antagonist; ND, transcript not detectable in ≥2 of 4 replicates; ns, not significant; PDCD1LG2, programmed cell death 1 ligand 2; TGFB1, transforming growth factor beta 1; TGFB2, transforming growth factor beta 2. *$p < 0.05$, **$p < 0.01$, ***$p < 0.001$, ****$p < 0.0001$.

gene transcripts changed significantly in one or more donor isolates, including changes in CCL2, immunoglobulin superfamily adhesion molecules (ICAM1 or VCAM1), and programmed death ligand (CD274 and/or PDCD1LG2)

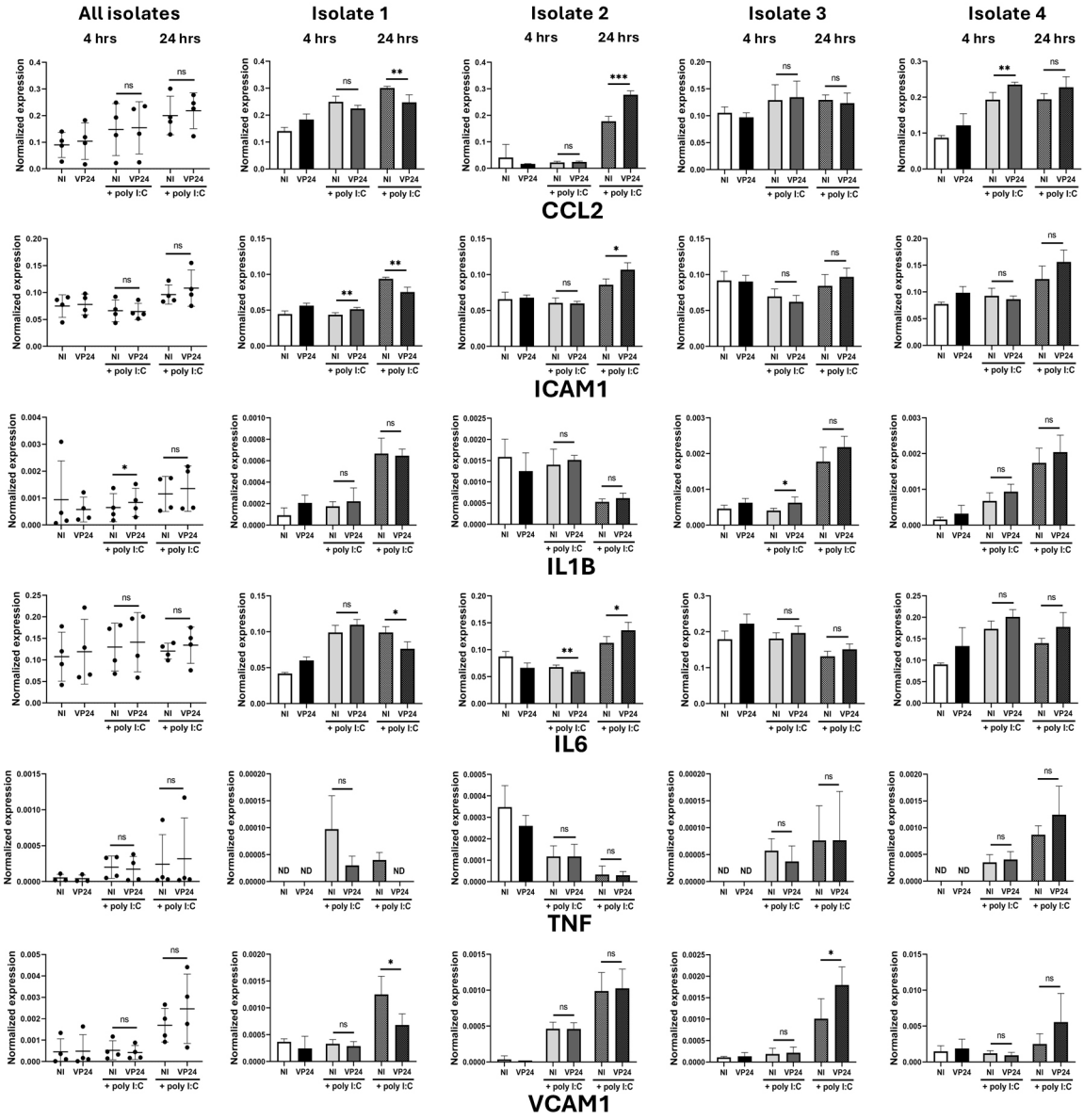

Figure 5. Expression of proinflammatory gene transcripts in human retinal pigment epithelial cells. After transfection with *Zaire ebolavirus* viral protein 24 (VP24) or no-insert control (NI) expression plasmid for 48 h, followed by polyinosinic-polycytidylic acid (poly I:C) for an additional 4 or 24 h (hours), cellular levels of levels of six proinflammatory gene transcripts were measured by quantitative polymerase chain reaction and normalized to two stable reference genes (glyceraldehyde 3-phosphate dehydrogenase [GAPDH] and peptidylprolyl isomerase A [PPIA]). An additional control replacing poly I:C with water was included for the 4-h condition. In *All Isolate* graphs, circles represent mean expression in individual isolates, crossbars indicate mean, and error bars indicate standard deviation (n = 4 isolates/condition). In *Isolate 1–4* graphs, bars indicate mean normalized expression, and error bars indicate standard deviation (n = 4 replicates/condition). CCL2, C-C motif chemokine ligand 2; ICAM1, intercellular adhesion molecule 1; IL1B, interleukin 1 beta; IL6, interleukin 6; ND, transcript not detectable in ≥2 of 4 replicates; ns, not significant; TNF, tumor necrosis factor; VCAM1, vascular cell adhesion molecule 1. *$p < 0.05$, **$p < 0.01$, ***$p < 0.001$, ****$p < 0.0001$.

transcripts in three of the four donor isolates. Changes in all these molecules in retinal pigment epithelial cells would be expected to impact the activation status of leukocytes in the event that the eye was infiltrated in the context of EBOV infection [36–38]. The retinal pigment epithelium is a major contributor to ocular immune privilege in the posterior segment of the eye and acts to limit intraocular inflammation in most settings by upregulating immunomodulatory signals and downregulating proinflammatory signals [39]. However, a proinflammatory effect has been demonstrated in *Toxoplasma gondii* infection [14], and thus the opposite is also possible.

The donor-associated differences in molecular responses in our study, illustrated by multidimensional scaling and evident across the different individual molecular results, are notable. This is a phenomenon we have observed in studies of other primary human ocular cell populations, including iris pigment epithelial cells [40], retinal endothelial cells [41], and retinal Müller glial cells (manuscript in press), as well as retinal pigment epithelial cells [28]. It may be relevant to disease pathology as this occurs in individual patients. Although a common complication, most Ebola survivors do not develop uveitis: cohort studies indicate that approximately 10% to 35% of Ebola survivors have uveitis [2–4]. Moreover, considering detailed descriptions of the uveitis specifically, it is clear that this condition has quite varied manifestations among patients, including in relation to location within the eye (i.e., anterior, intermediate, anterior/intermediate, posterior, and pan - uveitis), unilateral and bilateral involvement, and associated features (e.g., corneal edema, posterior synechiae, intraretinal fluid, and ocular hypertension) [5,7,9]. Multiple clinical factors contribute to this broad spectrum of pathology across patients, including medical comorbidities and the management approach to the acute infection [42]. Another variable might be the individual molecular responses of ocular cell populations, including the retinal pigment epithelium, to infection with EBOV, and to EBOV VP24 specifically as studied here.

Studies of EBOV VP24 activity are conducted largely in human cell lines—most commonly human embryonic kidney HEK293 cells and human hepatoma Huh7 cells [43–46]. Interestingly, in their study of EBOV viral proteins in primary human dendritic cells, Ilinykh et al. [47] observed a relatively limited effect of mutating VP24 on host cell gene expression, in comparison to VP35, and with variation between the two cell isolates that were studied. Variation in the response of different cell populations to infection with EBOV was demonstrated conclusively in comprehensive single-cell profiling analysis of multiple leukocyte subsets isolated from EBOV-infected rhesus monkeys [48]. Taken together, these observations indicate it is plausible that activity of VP24 cells in the standard cell lines used to interrogate its mechanisms differs from its activity in primary human retinal pigment epithelial cells and potentially primary human cells in general.

In summary, our findings suggest that VP24 elicits a variable immune response from human retinal pigment epithelial cells, a primary EBOV target cell population in the eye, potentially contributing to the variable clinical presentation of post-Ebola uveitis in patients. Our work is limited by its in vitro nature but draws strength from the use of human primary cell isolates. Future research could compare the activity of EBOV VP24 with other filovirus VP24 on host immune responses. Importantly, we hope that this work stimulates interest in the use of primary human cells, including cells from other immune-privileged body sites, in studies of VP24 activity in Ebola virus disease.

APPENDIX 1. SUPPLEMENTARY TABLE 1.

To access the data, click or select the words "Appendix 1."

APPENDIX 2. SUPPLEMENTARY FIGURE 1.

To access the data, click or select the words "Appendix 2."

ACKNOWLEDGMENTS

The authors wish to thank Ms. Janet Matthews for administrative support in preparing this manuscript. Funding: This work was supported in part by an Investigator Grant (2025222 to JRS) and a Project Grant (1139857 to JRS, GAM and SY) from the National Health and Medical Research Council (Australia). Author contributions: Conceptualization: SY, GAM, JRS; Bibliographic research: CDH, SY, JRS; Methodology: LMA, YM, BA, GFO, GAM, JRS; Statistical analyses: LMA; Visualizations: LMA; Drafting of manuscript: LMA, JRS; Review and editing of manuscript: YM, BA, GFO, CDH, SY, GAM; Supervision: BA, GAM, JRS. Competing interests statement: The authors declare no competing interests. Data availability statement: All data generated or analyzed during this study are included in this published article.

REFERENCES

1. Kaner J, Schaack S. Understanding Ebola: the 2014 epidemic. Global Health 2016; 12:53-[PMID: 27624088].

2. Tiffany A, Vetter P, Mattia J, Dayer JA, Bartsch M, Kasztura M, Sterk E, Tijerino AM, Kaiser L, Ciglenecki I. Ebola virus disease complications as experienced by survivors in Sierra Leone. Clin Infect Dis 2016; 62:1360-6. [PMID: 27001797].

3. . The PREVAIL III Study Group. Sneller MC, Reilly C, Badio M, Bishop RJ, Eghrari AO, Moses SJ, Johnson KL, Gayedyu-Dennis D, Hensley LE, Higgs ES, Nath A, Tuznik K, Varughese J, Jensen KS, Dighero-Kemp B, Neaton JD, Lane HC, Fallah MP. A longitudinal study of Ebola sequelae in Liberia. N Engl J Med 2019; 380:924-34. .

4. Choo CH, Ward L, Crozier I, Fashina T, Yan D, Hayek BR, Hartley C, Vandy M, Mattia JG, Harrison-Williams L, Mustapha J, Drews-Botsch C, Yeh S, Shantha J. Ophthalmic sequelae of Ebola virus disease in survivors, Sierra Leone. Emerg Infect Dis 2024; 30:2502-9. [PMID: 39592396].

5. Shantha JG, Crozier I, Hayek BR, Bruce BB, Gargu C, Brown J, Fankhauser J, Yeh S. Ophthalmic manifestations and causes of vision impairment in Ebola virus disease survivors in Monrovia, Liberia. Ophthalmology 2017; 124:170-7. [PMID: 27914832].

6. Berry DE, Bavinger JC, Fernandes A, Mattia JG, Mustapha J, Harrison-Williams L, Teshome M, Vandy MJ, Shantha JG, Yeh S. Ebola Virus Persistence in Ocular Tissues and Fluids (EVICT) Study Investigators. Posterior segment ophthalmic manifestations in Ebola survivors, Sierra Leone. Ophthalmology 2021; 128:1371-3. [PMID: 33561480].

7. Hereth-Hebert E, Bah MO, Etard JF, Sow MS, Resnikoff S, Fardeau C, Toure A, Ouendeno AN, Sagno IC, March L, Izard S, Lama PL, Barry M, Delaporte E. Postebogui Study Group. Ocular complications in survivors of the Ebola outbreak in Guinea. Am J Ophthalmol 2017; 175:114-21. [PMID: 27998698].

8. Steptoe PJ, Scott JT, Baxter JM, Parkes CK, Dwivedi R, Czanner G, Vandy MJ, Momorie F, Fornah AD, Komba P, Richards J, Sahr F, Beare NAV, Semple MG. Novel retinal lesion in Ebola survivors, Sierra Leone, 2016. Emerg Infect Dis 2017; 23:1102-9. [PMID: 28628441].

9. Eghrari AO, Bishop RJ, Ross RD, Davis B, Larbelee J, Amegashie F, Dolo RF, Prakalapakorn SG, Gaisie C, Gargu C, Sosu Y, Sackor J, Cooper PZ, Wallace A, Nyain R, Gray M, Kamara F, Burkholder B, Brady CJ, Ray V, Tawse KL, Yeung I, Neaton JD, Higgs ES, Lane HC, Reilly C, Sneller MC, Fallah MP. Characterization of Ebola virus-associated eye disease. JAMA Netw Open 2021; 4:e2032216[PMID: 33399856].

10. Mochizuki M, Sugita S, Kamoi K. Immunological homeostasis of the eye. Prog Retin Eye Res 2013; 33:10-27. [PMID: 23108335].

11. Allart S, Lulé J, Serres B, Jones T, Davignon JL, Malecaze F, Davrinche C. Impaired killing of HCMV-infected retinal pigment epithelial cells by anti-pp65 CD8(+) cytotoxic T cells. Invest Ophthalmol Vis Sci 2003; 44:665-71. [PMID: 12556397].

12. Graybill C, Claypool DJ, Brinton JT, Levin MJ, Lee KS. Cytokines produced in response to varicella-zoster virus infection of ARPE-19 cells stimulate lymphocyte chemotaxis. J Infect Dis 2017; 216:1038-47. [PMID: 28968855].

13. La Distia Nora R, Walburg KV, van Hagen PM, Swagemakers SMA, van der Spek PJ, Quinten E, van Velthoven M, Ottenhoff THM, Dik WA, Haks MC. Retinal pigment epithelial cells control early *Mycobacterium tuberculosis* infection via interferon signaling. Invest Ophthalmol Vis Sci 2018; 59:1384-95. [PMID: 29625462].

14. Smith JR, Ashander LM, Arruda SL, Cordeiro CA, Lie S, Rochet E, Belfort R Jr, Furtado JM. Pathogenesis of ocular toxoplasmosis. Prog Retin Eye Res 2021; 81:100882[PMID: 32717377].

15. Todd S, Ma Y, Ashander LM, Appukuttan B, Michael MZ, Blenkinsop TA, Yeh S, Marsh GA, Smith JR. Ebola virus differentially infects human iris and retinal pigment epithelial cells. Front Virol 2022; 2:892394.

16. Messaoudi I, Amarasinghe GK, Basler CF. Filovirus pathogenesis and immune evasion: insights from Ebola virus and Marburg virus. Nat Rev Microbiol 2015; 13:663-76. [PMID: 26439085].

17. Jacob ST, Crozier I, Fischer WA 2nd, Hewlett A, Kraft CS, Vega MA, Soka MJ, Wahl V, Griffiths A, Bollinger L, Kuhn JH. Ebola virus disease. Nat Rev Dis Primers 2020; 6:13-[PMID: 32080199].

18. McNab F, Mayer-Barber K, Sher A, Wack A, O'Garra A. Type I interferons in infectious disease. Nat Rev Immunol 2015; 15:87-103. [PMID: 25614319].

19. Smith LM, Hensley LE, Geisbert TW, Johnson J, Stossel A, Honko A, Yen JY, Geisbert J, Paragas J, Fritz E, Olinger G, Young HA, Rubins KH, Karp CL. Interferon-β therapy prolongs survival in rhesus macaque models of Ebola and Marburg hemorrhagic fever. J Infect Dis 2013; 208:310-8. [PMID: 23255566].

20. Reid SP, Valmas C, Martinez O, Sanchez FM, Basler CF. Ebola virus VP24 proteins inhibit the interaction of NPI-1 subfamily karyopherin alpha proteins with activated STAT1. J Virol 2007; 81:13469-77. [PMID: 17928350].

21. Smith JR, Todd S, Ashander LM, Charitou T, Ma Y, Yeh S, Crozier I, Michael MZ, Appukuttan B, Williams KA, Lynn DJ, Marsh GA. Retinal pigment epithelial cells are a potential reservoir for Ebola virus in the human eye. Transl Vis Sci Technol 2017; 6:12-[PMID: 28721309].

22. Strunnikova NV, Maminishkis A, Barb JJ, Wang F, Zhi C, Sergeev Y, Chen W, Edwards AO, Stambolian D, Abecasis G, Swaroop A, Munson PJ, Miller SS. Transcriptome analysis and molecular signature of human retinal pigment epithelium. Hum Mol Genet 2010; 19:2468-86. [PMID: 20360305].

23. Schwarz TM, Edwards MR, Diederichs A, Alinger JB, Leung DW, Amarasinghe GK, Basler CF. VP24-karyopherin alpha binding affinities differ between Ebolavirus species, influencing interferon inhibition and VP24 stability. J Virol 2017; 91:91-[PMID: 27974555].

24. Smith JR, Ashander LM, Ma Y, Rochet E, Furtado JM. Model systems for studying mechanisms of ocular toxoplasmosis. Methods Mol Biol 2020; 2071:297-321. [PMID: 31758460].

25. Pfaffl MW. A new mathematical model for relative quantification in real-time RT-PCR. Nucleic Acids Res 2001; 29:e45[PMID: 11328886].

26. Ashander LM, Lumsden AL, Dawson AC, Ma Y, Ferreira LB, Oliver GF, Appukuttan B, Carr JM, Smith JR. Infection of human retinal pigment epithelial cells with dengue virus strains isolated during outbreaks in Singapore. Microorganisms 2022; 10:310-[PMID: 35208767].

27. Carr JM, Ashander LM, Calvert JK, Ma Y, Aloia A, Bracho GG, Chee SP, Appukuttan B, Smith JR. Molecular responses of human retinal cells to infection with dengue virus. Mediators Inflamm 2017; 2017:3164375[PMID: 29515292].

28. Lie S, Rochet E, Segerdell E, Ma Y, Ashander LM, Shadforth AMA, Blenkinsop TA, Michael MZ, Appukuttan B, Wilmot B, Smith JR. Immunological molecular responses of human retinal pigment epithelial cells to infection with *Toxoplasma gondii*. Front Immunol 2019; 10:708-[PMID: 31118929].

29. Daugherty MD, Malik HS. How a virus blocks a cellular emergency access lane to the nucleus, STAT! Cell Host Microbe 2014; 16:150-2. [PMID: 25121743].

30. Kato H, Oh SW, Fujita T. RIG-I-like receptors and type I interferonopathies. J Interferon Cytokine Res 2017; 37:207-13. [PMID: 28475461].

31. Carey CM, Govande AA, Cooper JM, Hartley MK, Kranzusch PJ, Elde NC. Recurrent loss-of-function mutations reveal costs to OAS1 antiviral activity in primates. Cell Host Microbe 2019; 25:336-343.e4. [PMID: 30713099].

32. Rivera-Serrano EE, Gizzi AS, Arnold JJ, Grove TL, Almo SC, Cameron CE. Viperin reveals its true function. Annu Rev Virol 2020; 7:421-46. [PMID: 32603630].

33. García MA, Meurs EF, Esteban M. The dsRNA protein kinase PKR: virus and cell control. Biochimie 2007; 89:799-811. [PMID: 17451862].

34. Mears HV, Sweeney TR. Better together: the role of IFIT protein-protein interactions in the antiviral response. J Gen Virol 2018; 99:1463-77. [PMID: 30234477].

35. Álvarez E, Falqui M, Sin L, McGrail JP, Perdiguero B, Coloma R, Marcos-Villar L, Tárrega C, Esteban M, Gómez CE, Guerra S. Unveiling the multifaceted roles of ISG15: from immunomodulation to therapeutic frontiers. Vaccines (Basel) 2024; 12:153-[PMID: 38400136].

36. Gschwandtner M, Derler R, Midwood KS. More than just attractive: how CCL2 influences myeloid cell behavior beyond chemotaxis. Front Immunol 2019; 10:2759-[PMID: 31921102].

37. Haydinger CD, Ashander LM, Tan ACR, Smith JR. Intercellular adhesion molecule 1: more than a leukocyte adhesion molecule. Biology (Basel) 2023; 12:743-[PMID: 37237555].

38. Burke KP, Chaudhri A, Freeman GJ, Sharpe AH. The B7:CD28 family and friends: Unraveling coinhibitory interactions. Immunity 2024; 57:223-44. [PMID: 38354702].

39. Du Y, Yan B. Ocular immune privilege and retinal pigment epithelial cells. J Leukoc Biol 2023; 113:288-304. [PMID: 36805720].

40. Ryan FJ, Carr JM, Furtado JM, Ma Y, Ashander LM, Simões M, Oliver GF, Granado GB, Dawson AC, Michael MZ, Appukuttan B, Lynn DJ, Smith JR. Zika virus infection of human iris pigment epithelial cells. Front Immunol 2021; 12:644153[PMID: 33968035].

41. Ryan FJ, Ma Y, Ashander LM, Kvopka M, Appukuttan B, Lynn DJ, Smith JR. Transcriptomic responses of human retinal vascular endothelial cells to inflammatory cytokines. Transl Vis Sci Technol 2022; 11:27-[PMID: 36018584].

42. Malvy D, McElroy AK, de Clerck H, Günther S, van Griensven J. Ebola virus disease. Lancet 2019; 393:936-48. [PMID: 30777297].

43. Xu W, Edwards MR, Borek DM, Feagins AR, Mittal A, Alinger JB, Berry KN, Yen B, Hamilton J, Brett TJ, Pappu RV, Leung DW, Basler CF, Amarasinghe GK. Ebola virus VP24 targets a unique NLS binding site on karyopherin alpha 5 to selectively compete with nuclear import of phosphorylated STAT1. Cell Host Microbe 2014; 16:187-200. [PMID: 25121748].

44. Takamatsu Y, Kolesnikova L, Becker S. Ebola virus proteins NP, VP35, and VP24 are essential and sufficient to mediate nucleocapsid transport. Proc Natl Acad Sci U S A 2018; 115:1075-80. [PMID: 29339477].

45. He FB, Khan H, Huttunen M, Kolehmainen P, Melén K, Maljanen S, Qu M, Jiang M, Kakkola L, Julkunen I. Filovirus VP24 proteins differentially regulate RIG-I and MDA5-dependent type I and III interferon promoter activation. Front Immunol 2022; 12:694105[PMID: 35069519].

46. Vogel OA, Nafziger E, Sharma A, Pasolli HA, Davey RA, Basler CF. The role of Ebola virus VP24 nuclear trafficking signals in infectious particle production. BioArch. 2024; xxx:584761.

47. Ilinykh PA, Lubaki NM, Widen SG, Renn LA, Theisen TC, Rabin RL, Wood TG, Bukreyev A. Different temporal effects of Ebola virus VP35 and VP24 proteins on global gene expression in human dendritic cells. J Virol 2015; 89:7567-83. [PMID: 25972536].

48. Kotliar D, Lin AE, Logue J, Hughes TK, Khoury NM, Raju SS, Wadsworth MH 2nd, Chen H, Kurtz JR, Dighero-Kemp B, Bjornson ZB, Mukherjee N, Sellers BA, Tran N, Bauer MR, Adams GC, Adams R, Rinn JL, Melé M, Schaffner SF, Nolan GP, Barnes KG, Hensley LE, McIlwain DR, Shalek AK, Sabeti PC, Bennett RS. Single-cell profiling of Ebola virus disease in vivo reveals viral and host dynamics. Cell 2020; 183:1383-1401.e19. [PMID: 33159858].

49. Oliver GF, Ashander LM, Dawson AC, Ma Y, Carr JM, Williams KA, Smith JR. Dengue virus infection of human retinal Müller glial cells. Viruses 2023; 15:1410-[PMID: 37515098].

50. Hu CW, Yin GF, Wang XR, Ren BW, Zhang WG, Bai QL, Lv YM, Li WL, Zhao WQ. IL-24 induces apoptosis via upregulation of RNA-activated protein kinase and enhances temozolomide-induced apoptosis in glioma cells. Oncol Res 2014; 22:159-65. [PMID: 26168134].

51. Lu CY, Yang YC, Li CC, Liu KL, Lii CK, Chen HW. Andrographolide inhibits TNFα-induced ICAM-1 expression via suppression of NADPH oxidase activation and induction of HO-1 and GCLM expression through the PI3K/Akt/Nrf2

and PI3K/Akt/AP-1 pathways in human endothelial cells. Biochem Pharmacol 2014; 91:40-50. [PMID: 24998495].

52. Sharma N, Verma R, Kumawat KL, Basu A, Singh SK. miR-146a suppresses cellular immune response during Japanese encephalitis virus JaOArS982 strain infection in human microglial cells. J Neuroinflammation 2015; 12:30-[PMID: 25889446].

53. Warren CJ, Griffin LM, Little AS, Huang IC, Farzan M, Pyeon D. The antiviral restriction factors IFITM1, 2 and 3 do not inhibit infection of human papillomavirus, cytomegalovirus and adenovirus. PLoS One 2014; 9:e96579[PMID: 24827144].

54. Blengio F, Raggi F, Pierobon D, Cappello P, Eva A, Giovarelli M, Varesio L, Bosco MC. The hypoxic environment reprograms the cytokine/chemokine expression profile of human mature dendritic cells. Immunobiology 2013; 218:76-89. [PMID: 22465745].

55. Eftekharian MM, Ghafouri-Fard S, Noroozi R, Omrani MD, Arsang-Jang S, Ganji M, Gharzi V, Noroozi H, Komaki A, Mazdeh M, Taheri M. Cytokine profile in autistic patients. Cytokine 2018; 108:120-6. [PMID: 29602155].

56. Muscat P, Mercado K, Payne K, Chahal H, Jones G. PHF11 expression and cellular distribution is regulated by the Toll-Like Receptor 3 Ligand Polyinosinic:Polycytidylic Acid in HaCaT keratinocytes. BMC Immunol 2015; 16:69-[PMID: 26573531].

57. Wang B, Zhao XP, Fan YC, Zhang JJ, Zhao J, Wang K. IL-17A but not IL-22 suppresses the replication of hepatitis B virus mediated by over-expression of MxA and OAS mRNA in the HepG2.2.15 cell line. Antiviral Res 2013; 97:285-92. [PMID: 23274784].

58. Hobo W, Maas F, Adisty N, de Witte T, Schaap N, van der Voort R, Dolstra H. siRNA silencing of PD-L1 and PD-L2 on dendritic cells augments expansion and function of minor histocompatibility antigen-specific CD8+ T cells. Blood 2010; 116:4501-11. [PMID: 20682852].

59. Reins RY, Baidouri H, McDermott AM. Vitamin D activation and function in human corneal epithelial cells during TLR-induced inflammation. Invest Ophthalmol Vis Sci 2015; 56:7715-27. [PMID: 26641549].

60. Wang B, Fang Y, Wu Y, Koga K, Osuga Y, Lv S, Chen D, Zhu Y, Wang J, Huang H. Viperin is induced following toll-like receptor 3 (TLR3) ligation and has a virus-responsive function in human trophoblast cells. Placenta 2015; 36:667-73. [PMID: 25814471].

61. Jang CH, Choi JH, Byun MS, Jue DM. Chloroquine inhibits production of TNF-alpha, IL-1beta and IL-6 from lipopolysaccharide-stimulated human monocytes/macrophages by different modes. Rheumatology (Oxford) 2006; 45:703-10. [PMID: 16418198].

62. Silverman MD, Zamora DO, Pan Y, Texeira PV, Baek SH, Planck SR, Rosenbaum JT. Constitutive and inflammatory mediator-regulated fractalkine expression in human ocular tissues and cultured cells. Invest Ophthalmol Vis Sci 2003; 44:1608-15. [PMID: 12657599].

Articles are provided courtesy of Emory University and The Abraham J. & Phyllis Katz Foundation. The print version of this article was created on 4 February 2026. This reflects all typographical corrections and errata to the article through that date. Details of any changes may be found in the online version of the article.